clear Instruments and Methods 205 (1983) 99–105
rth-Holland Publishing Company

SILICON COUNTER TELESCOPE TO STUDY SHORT-LIVED PARTICLES IN IGH-ENERGY HADRONIC INTERACTIONS

HYAMS and U. KOETZ *
RN, Geneva, Switzerland

BELAU, R. KLANNER, G. LUTZ, E. NEUGEBAUER and A. WYLIE
x-Planck-Institut für Physik und Astrophysik, Werner-Heisenberg-Institut, Munich, Fed. Rep. Germany

KEMMER
hnische Universität, Munich, Fed. Rep. Germany

ceived 5 July 1982

A telescope consisting of six silicon microstrip detectors achieving 5 μm spatial resolution for minimum ionizing particles has been lt. The design and fabrication of the counters, electronics, and mechanical set-up is described, and first results of its performance in 75 GeV/c beam are reported.

Introduction

The telescope described in this article has been built an experiment to study the production and proper- s of charmed particles in 100–200 GeV hadronic eractions in a beryllium target at the CERN Super oton Synchrotron (SPS) **. The lifetime of charmed rticles of a few times 10^{-13} s, their production cross- tions of a few microbarns, and the general features of dronic interactions in this energy range, such as the arged multiplicity of ~ 10 and the concentration of st of the particles in a narrow forward cone, have fined the required performance of the counters:
spatial resolution of $\leqslant 10$ μm;
two-particle separation of ~ 120 μm in the region of highest particle density;
rate capability of approximately 10^6 per second;
minimal material to avoid multiple scattering, sec- ondary interactions, and photon conversion.
e have developed silicon microstrip detectors [1,2], ich have achieved this performance. In the following will describe their principle of operation, the fabrica- n of the detectors, the electronics used to read them as well as first test results in a high-energy beam.

2. The silicon microstrip detectors

2.1. Principles of operation

Fig. 1 shows schematically a cross-section of the detector. The basic material is a high-ohmic (~ 2 kΩ · cm) n-doped silicon crystal, 2 inches in diameter and 280 μm thick. One face of the crystal in aluminized. On the other face, the sensitive area of the counter (a rectangle of 24 mm × 36 mm in our case) is covered with p^+ implanted diode strips (1200 strips of 12 μm × 36 mm and 20 μm pitch) and Al contacts. Connecting the strips to a negative voltage of 160 V depletes the n-doped silicon crystal of free charge carriers, leaving behind the ionized dopant atoms, which produce an electric field decreasing linearly with the distance from the junction.

A relativistic particle of charge one traversing the 280 μm thick detector produces ~ 25000 electron–hole pairs which are collected within < 10 ns at the electrodes. The signal picked up at the readout strip yields the information on the particle trajectory to a precision determined by the pitch of the strips *.

The principle of charge division has been used to reduce the number of electronic channels: not every

Visitor from DESY, Hamburg, Fed. Rep. Germany.
NA11 Experiment at CERN (Amsterdam–Bristol–CERN–Cracow–MPI Munich–Rutherford Lab. Collaboration).

* Other effects come in at the level of a few μm:
- delta electrons: 90% of tracks will have a shift of the centre of gravity of the deposed charge of less than 2 μm;
- diffusion of charge carriers: < 1 μm.

5087/83/0000–0000/$03.00

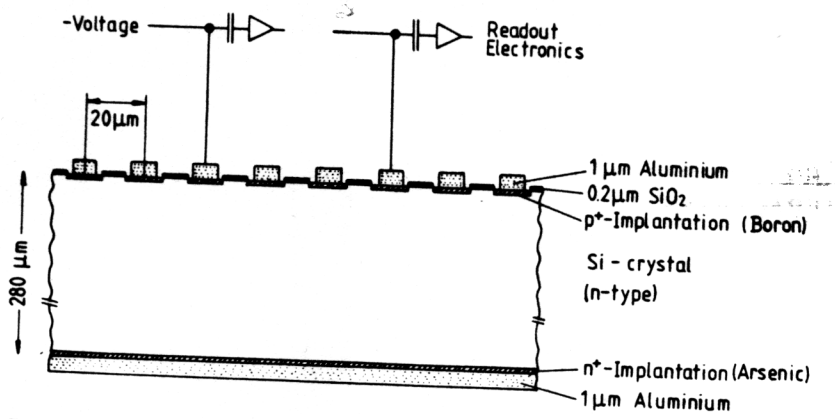

Fig. 1. Cross-section of a microstrip detector with capacitative charge division.

strip is connected to readout electronics. The charge collected at intermediate strips is divided amongst the neighbouring strips via the interstrip capacitances (fig. 1).

For capacitative charge division to work, several conditions have to be met:

- for uniform charge collection, the intermediate strips have to be kept at the potential of the readout strips;
- to avoid cross-talk, the impedance between readout strips has to be significantly larger than the dynamic input impedance of the electronics;
- to avoid signal losses to ground, the interstrip capacitance has to be big compared to the strip-to-ground capacitance.

The advantage of the charge division method is the significant reduction in the number of electronics channels. However, it needs low noise analogue electronics and yields worse two-particle separation and pulse-height measurement than the direct readout of every channel.

2.2. Fabrication

Single, high-ohmic (~ 2 k$\Omega \cdot$cm) phosphor-doped crystals of silicon, 2 inches in diameter and 280 μm thick, are used as the base material. Table 1 lists the specifications of the crystal in more detail. The sensitive area of the counter, of 24 mm $\times$ 36 mm, is defined by

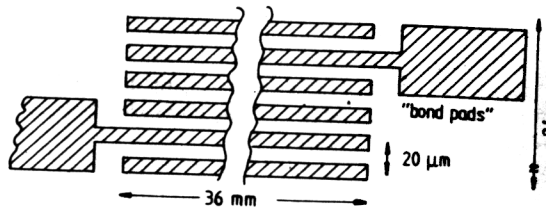

Fig. 2. Pattern of strips and bond pads for microstrip detect

the pattern of strips and bond pads shown in fig. 2.

The detectors are produced according to the techno ogy developed earlier by Kemmer [3] for coarser stru tures. The individual production steps are:

- growth of 0.2 μm of SiO_2 by thermal oxidation 1040°C;
- opening of the diode windows by photolithograph etching;
- implantation of the p^+ strips by bombardment wit 5×10^{14} B ions per cm^2 at 15 keV;
- implantation of the n^+ contact by bombardmen with 5×10^{15} As ions per cm^2 at 30 keV;
- thermal curing of the crystal at 600°C;
- evaporation of ~ 1 μm of Al onto both surfaces;
- photolithographic etching of the strip pattern;
- ion beam sputtering of a 1 mm wide Si strip trans

Table 1
Specifications of silicon crystals.

Dislocation-free, single crystals	orientation 1-1-1
Zone-refined, phosphor-doped resistance	> 2 k$\Omega \cdot$cm
Lifetime of charges	> 1 ms
One side polished/one side damage-free etching	
Dimensions	2″ $\pm$ 0.4 mm/280 $\pm$ 20 μm

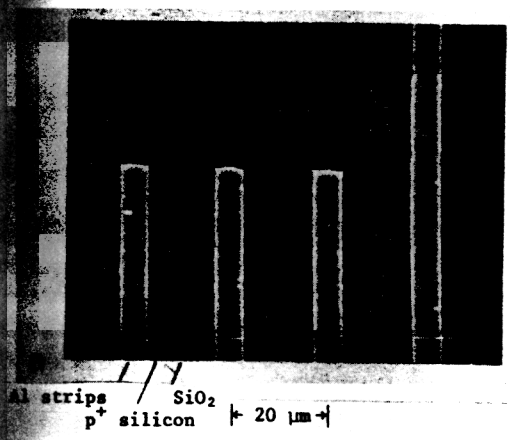

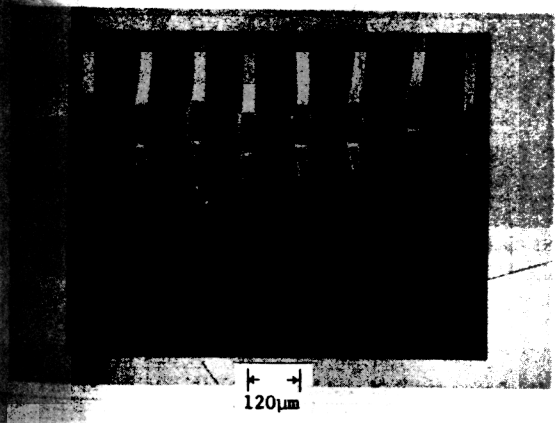

Fig. 3. (a) Electron micrograph of strips. (b) Electron micrograph of bond pads and bondings.

verse to the diode strips to obtain a 300 kΩ interstrip resistance.

Fig. 1 shows a cross-section through a finished detector; fig. 3a shows an electron micrograph of the strips. The Al strips and SiO_2 windows can be clearly seen, and the quality of the photolithographic etching as well as the precision of the mask alignment can be judged.

2.3. Mounting

For the use of the detectors in the experiment, the mechanical mounting has to fulfil the following requirements:

- parallelism of strips of several detectors within ±2 μm over 36 mm;
- parallelism of the detector planes within ± 15 μm;
- fanning out of the signal lines from 60 μm pitch on the detector to 1/20 of an inch;
- electrical shielding of the detectors.

The mechanical precision is obtained by gluing the 2 inch silicon crystal to a 100 mm × 100 mm × 1 mm quartz plate with a 48 mm diameter hole in the centre. This plate is in turn aligned and glued under a microscope to a precision quartz frame, 120 mm × 130 mm × 14 mm, with an 80 mm hole in the centre. The relative alignment of the detectors is achieved by clamping the quartz frames onto a granite optical bench and separating them by means of gauge blocks.

For fanning out the signals, a printed fibre board with 60 μm wide Cu-lines and a pitch changing from 120 μm to 1/20 of an inch, with a hole in the centre for the counter, is glued to the quartz frame. The connections between the bond pads on the counter and the electrolytically goldplated lines on the fibre board are made with 25 μm diameter Al wire, using the technique of ultrasonic bonding (fig. 3b). Flexible wires are soldered to the fan-out plate in order to make the connection to the electronics with a minimum of mechanical strain. Fig. 4 shows a photograph of a mounted counter. Finally, 25 μm aluminized mylar foils are mounted on both sides of the detector to protect it mechanically, optically, and electrically.

3. The electronics

3.1. The amplifier chain

Fig. 5 shows a block diagram of the electronic chain. A hybridized charge-sensitive preamplifier, 10 mm × 30 mm × 3.5 mm, is followed by a shaping amplifier-driver, which drives a 40 m long, 110 Ω, twisted-pair cable. The preamplifier and the shaping amplifier boards for 12 channels are plugged into mother boards, which are mounted radially at a distance of 18 cm from the centre of the detector. The gain of this first stage is 40 mV/5 × 10^{-15} C (mean pulse height for minimum ionizing particles); the bipolar output pulse has a rise-time of 85 ns and a total duration of 850 ns. Twisted-pair cables, 40 m long, lead to the main amplifiers in the electronics barrack of the experiment. They have analog outputs for pulse-height recording and logic outputs for fast decision. The analog signals are further delayed by 60 m of twisted-pair cables and then coupled via transformers to the LRS-2281 voltage-sensitive ADCs.

The equivalent input r.m.s. noise of the entire chain amounts to 450 + 15 · C (pF) electrons, with C being the input capacitance (detector + leads) in pF. In the experimental set-up with the detector connected, the typical noise is 750 electrons.

The entire chain is linear for signals up to 2.5 minimum ionizing particles.

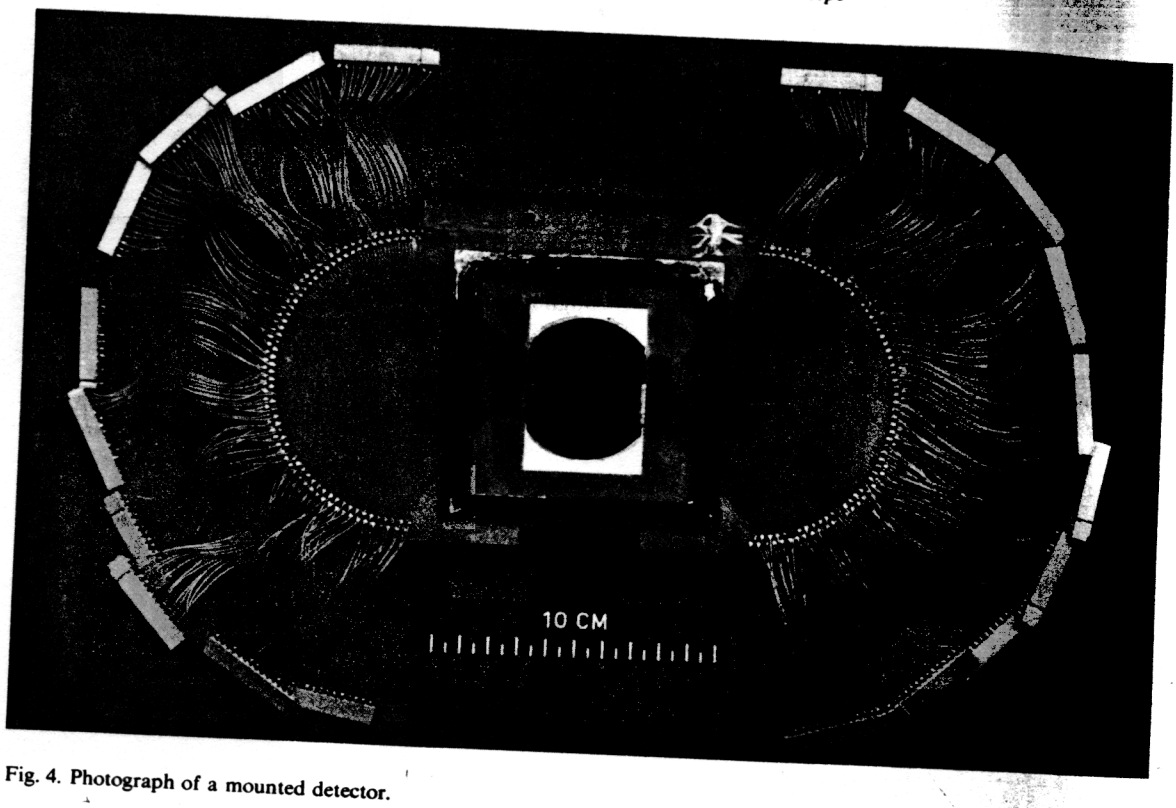

Fig. 4. Photograph of a mounted detector.

3.2. The calibration system

For setting up, monitoring, and calibrating the entire electronics chain, test signals of a few millivolts are injected via 1.2 pF capacitances into the input of the charge-sensitive amplifiers. Under computer control the amplitude of the calibration pulse can be varied for linearity measurement, and any combination of four different groups of amplifiers (right–left–even–odd) can be selected. The agreement between the calibration obtained from the test pulse system and minimum ionizing particles is within ± 10%.

4. Performance and results

4.1. Voltage–current characteristics

The voltage–current characteristics for a detector with all diodes connnected in parallel are shown in fig. 6. At the calculated voltage for full depletion, the dark current per readout strip is about 1 nA. This is a factor of 100 below the value at which the current would contribute noticeably to the electronics noise.

4.2. Measurements with 175 GeV/c π mesons

4.2.1. The set-up

Six detectors, mounted on quartz plates as described in section 2.3, were arranged on an optical bench in

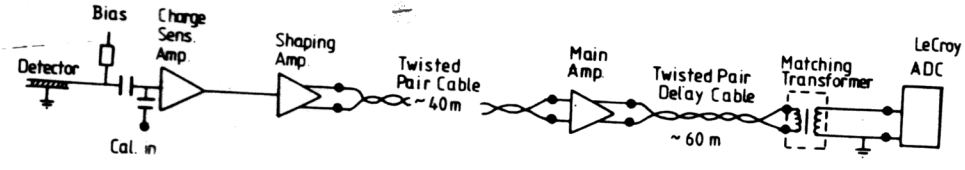

Fig. 5. Block diagram of the readout electronics.

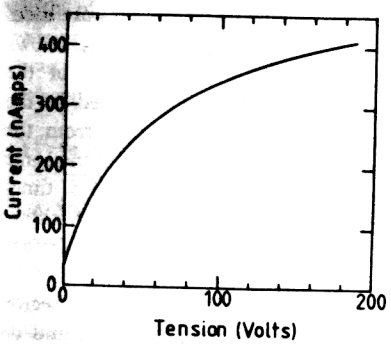

Fig. 6. Voltage/current characteristics of an entire detector.

three groups. Each group consists of two counters with an angle, between the strips and the horizontal, of $+14°$ and $-14°$. The distance between the two detectors in a pair was 8 mm, the distance between pairs was 44 mm. To each of the first two detectors, 120 channels of readout electronics were connected, and 240 channels to each of the remaining detectors, with readout every 60 μm in the central 4.8 mm and every 120 μm in the outer regions. The telescope was set up in the H6 beam of the CERN Super Proton Synchrotron (SPS) as part of the multiparticle spectrometer of the ACCMOR Collaboration (see footnote in sect. 1).

4.2.2. Response to 175 GeV/c π mesons

The beam was defined by a set of three scintillation counters, which provided gating signals for the ADCs. The gains of the individual electronics channels were normalized using the calibration system described in section 3.2. The passage of minimum ionizing particles produces clusters of pulse heights in adjacent strips of the detector. For the analysis, we define a cluster as being a group of adjacent channels with at least 0.1 times the most probable pulse height of minimum ionizing particles per strip and a total pulse height of the cluster exceeding 0.3 minimum ionizing particles.

Table 2 shows the number of clusters for single beam tracks. The numbers are insensitive to the exact criteria of the cluster definition. To avoid background from

Table 2
Number of clusters for beam tracks (10000 events).

No. of clusters	Fraction of events (%)
0	0
1	98.6
≥ 2	1.4

Table 3
Cluster size distribution for beam tracks (10000 events).

Cluster size	Fraction of events	
	60 μm region	120 μm region
1	0.24	0.16
2	0.46	0.51
3	0.22	0.26
≥ 4	0.08	0.07

interactions upstream of the counters and in the counters, we have required in this analysis that there be only one cluster in the five other detectors. With this condition the inefficiency of an individual detector is smaller than 2×10^{-4}, and the number of events with more than one cluster is about 1% – an order of magnitude expected from δ-electrons.

Table 3 shows the distribution of cluster size for the 60 μm and 120 μm readout regions. Naïvely, for the 60 μm region one expects one-third single clusters and two-thirds double clusters, and for the 120 μm region, one-sixth single and five-sixths double. Energetic δ-rays and capacitative coupling to non-adjacent readout channels contribute to the significant fraction of events with cluster size exceeding two.

Fig. 7 shows the pulse height for the cluster. Electronics noise, Landau fluctuations, difference in calibration, as well as differences in charge collection – depending on whether a readout strip or an interpolation strip was hit – contribute to the full width of approximately 50%.

4.2.3. Spatial resolution

A first approximation of the particle position is obtained from the centre of gravity of the cluster. If this value lies within ± 10 μm of a readout strip, the position is obtained from the centre of gravity of the three

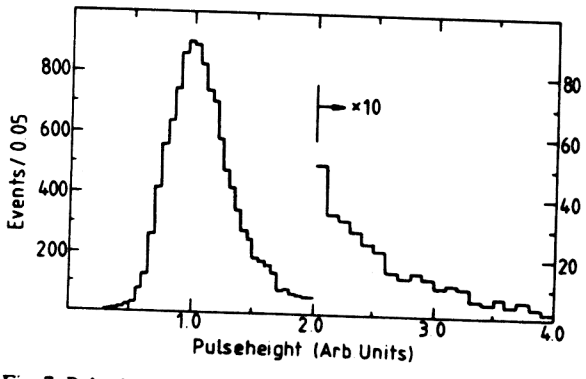

Fig. 7. Pulse-height distribution for minimum ionizing particles.

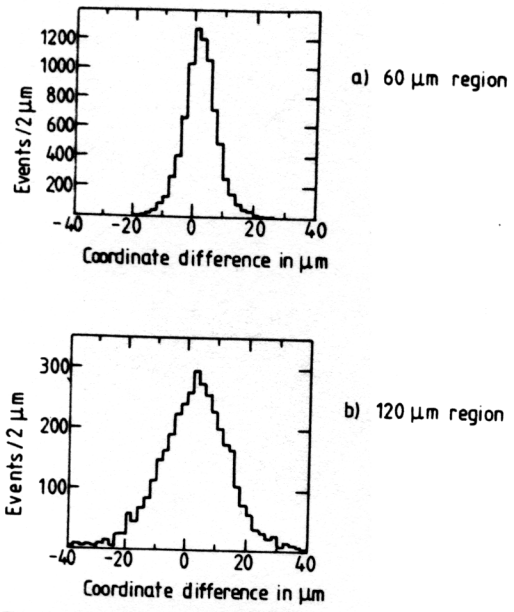

Fig. 8. Spatial resolution of the detectors. For the measurement, three detectors are mounted with parallel strips. The distribution of the difference between the position measured in the central detector and the position predicted from the two outer detectors is shown.

nearest strips, otherwise the two nearest strips are us

Having three counters with parallel strips allo direct determination of the spatial resolution of t detectors by comparing the position measured in t central detector with the position predicted from t outer planes. Assuming that all detectors have the sa resolution, the width of this distribution is $\sqrt{1.5}$ tim the resolution of the individual counter. Fig. 8 sho the measured distribution for the 60 μm and 120 μ regions separately. We deduce a spatial resolution of 4 μm and 7 μm. The resolution in the 120 μm regi depends critically on the exact gain calibration and c the understanding of the cross-talk and noise. We e pect to get an improvement in resolution in this regio

4.2.4. Spatial alignment

Having six detector planes measuring two proje tions allows a check of the parallelism of the strips i the individual views. An angular misalignment of 0.0 mrad (or 2 μm over the 36 mm wide counter) has bee determined.

4.2.5. Intensity related effects

Data have been taken with beam intensities betwee 3×10^4 and 3×10^6 particles per 1.5 s SPS spill. N degradation of the spatial resolution, as measured i section 4.2.3, has been found in the 60 μm region t which the beam is confined in the experiment. However owing to out-of-time tracks, there is an increase in th

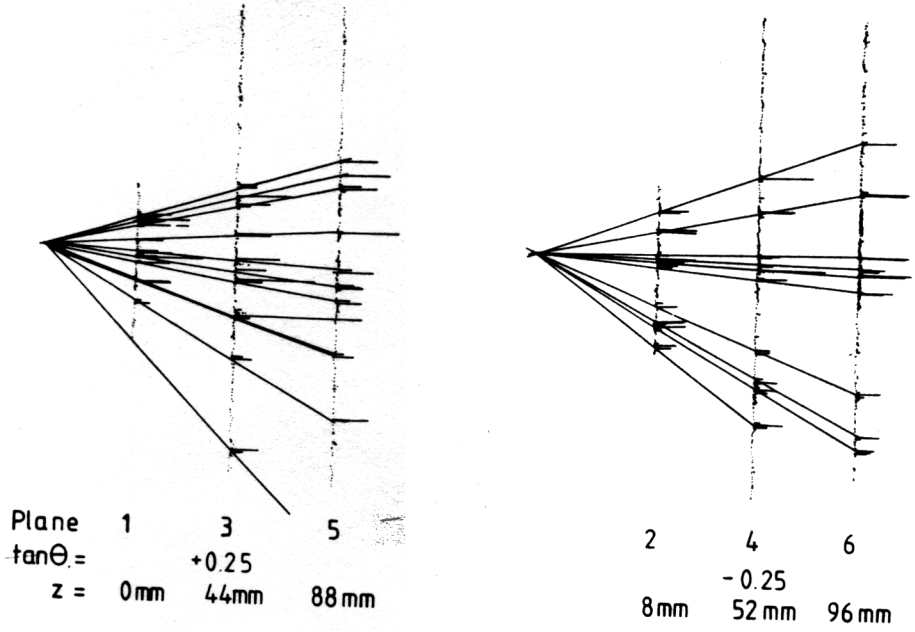

Fig. 9. On-line display of a 175 GeV/c π^- Be interaction measured in the six planes of the target telescope. The two projections, $\tan\theta = \pm 0.25$, are shown separately. Horizontal lines represent the pulse-height in the individual strips. The particle trajectories are also indicated.

width of the pulse-height distribution for minimum ionizing particles, an increase in inefficiency from 0 to about 10^{-3}, and an increase of double tracks by 20% between the low- and high-intensity data.

4.3. 175 GeV/c π^- Be interactions

A 20 mm long beryllium target was placed 40 mm in front of the first detector, and 175 GeV/c π^- Be interactions have been recorded. Fig. 9 shows an on-line display of an event. The two projections are shown separately to the right and left of the figure. The horizontal lines represent the pulse heights of the individual strips of the detectors. Lines corresponding to particle trajectories are also drawn. The work on reconstruction of multiparticle events and the determination of the precision of the vertex determination has only started.

5. Conclusions

A telescope of six silicon microstrip detectors with a spatial resolution of 5 μm has been built and successfully tested with high-energy particles.

We would like to end with the remark that high-precision silicon detectors of the type discussed in this paper have very severe limitations for use in high-energy experiments – in particular as central high-precision detectors for colliding beam experiments. For our counters the ratio of detector surface to the nearby electronics surface is approximately 1 : 300, which makes it impossible to cover large areas with detectors. We think that integrating electronics on the detector chip can solve this problem.

Many people have contributed to this project. We would like to thank, in particular, E. Aigner and G. Lindert from Siemens in Munich for making it possible to produce the precision photomasks; Messrs. A. Braem and C. Nichols from CERN and Dr. M. Königer and Mr. G. Reithmeier from MBB, Munich, for the sputtering of the surface resistivity. The high-precision mechanics were designed and built at the MPI, and we are especially grateful to Mr. P. Šolč for his dedicated and precise work in assembling the detectors. We thank Messrs. L. Hubbeling from CERN and W. Cwienk, W. Pimpl, H. Wenniger and P. Weißbach for the MPI for designing and building the electronics, and Dr. R. Richter from MPI for his contributions to the design and production of the fan-out plates. At all stages of the project we profited from the help of Messrs. E. Heijne and P. Jarron, CERN, whose equipment we used for early prototype tests; we are indebted to them for their contribution. This work would not have been possible without the strong support of all the members of the NAll Collaboration.

References

[1] E.H.M. Heijne et al., Nucl. Instr. and Meth. 178 (1980) 331, and refs. therein.
[2] J.B.A. England et al., Nucl. Instr. and Meth. 185 (1981) 43.
[3] J. Kemmer, Nucl. Instr. and Meth. 169 (1980) 449.